Journal of Alloys and Compounds 503 (2010) 416–421

Contents lists available at ScienceDirect

Journal of Alloys and Compounds

journal homepage: www.elsevier.com/locate/jallcom

Influences in high quality zinc oxide films and their photoelectrochemical performance

S.S. Shinde[a], Prakash S. Patil[b], R.S. Gaikwad[b], R.S. Mane[c], B.N. Pawar[b], K.Y. Rajpure[a,*]

[a] Electrochemical Materials Laboratory, Department of Physics, Shivaji University, Vidyanagar, Kolhapur, Maharashtra 416004, India
[b] Bharati Vidyapeeth Deemed University, Yashawantrao Mohite College, Pune-38, India
[c] Department of Physics, SRTM University, Nanded, India

ARTICLE INFO

Article history:
Received 11 December 2009
Received in revised form 4 May 2010
Accepted 5 May 2010
Available online 11 May 2010

Keywords:
Spray pyrolysis
Zinc oxide
Morphology
Optoelectronic properties
PEC performance

ABSTRACT

Transparent conductive zinc oxide thin films have been synthesized by spray pyrolytic decomposition of aqueous solution of zinc acetate onto the corning glasses with different pre-heating temperatures. The influence of pre-heating temperature on the structural, morphological, optoelectronic and electrical properties is investigated. The X-ray diffraction patterns revealed the polycrystalline nature with hexagonal (wurtzite) crystal structure. Films show preferred *c*-axis orientated with (0 0 2) growth. Films deposited at various deposition temperatures exhibit different surface morphologies. It is observed that the temperature plays an important role in modifying surface morphology and size of crystallites. Compact hexagonal platelets like structure is observed for lower temperature samples. The films exhibit nanoparticles of size 60–100 nm for 250–500 °C temperatures. Films are highly transparent and conducting, we achieved 95% transmittance at 550 nm with electrical resistivity 0.062 Ω cm and figure of merit 7.88×10^{-4} □/Ω. Moreover samples are photoelectrochemically active and exhibit the highest photocurrent of 212 μA, a photovoltage of 353 mV and 0.32 fill factor for the 450 °C films.

1. Introduction

The direct-band gap II–VI and III–V systems are of particular interest because of their high optoelectronic efficiencies relative to indirect-band gap of group IV elements. Zinc oxide is one of the most important group II–VI semiconductor materials. It is n-type wide-band gap oxide semiconductor with a direct energy gap of about 3.37 eV. Due to non-toxicity, higher abundance, thermal and mechanical stability zinc oxide is one of the most promising materials for the fabrication of the next generation of optoelectronic devices in the UV region. As a matter of fact, simultaneous occurrence of both high optical transmittance in the visible range, and low resistivity makes zinc oxide an important material in the manufacture of heat mirrors used in gas stoves, conducting coatings in aircrafts glasses to avoid surface icing, and thin film electrodes in amorphous silicon solar cells. Zinc oxide is a member of the hexagonal (wurtzite) class; it is a semiconducting, piezoelectric and optical wave guide material and has a variety of potential applications such as energy windows, liquid crystal displays, blue and ultraviolet (UV) light emitters [1], and transparent electrodes in solar cells, ultrasonic oscillators, bulk acoustic waves devices [2,3]. Alver et al. [4] had grown the ZnO microrods using the chemical spray pyrolysis technique at 600 °C. The spray solution was prepared by dissolving $ZnCl_2$ (2.73 g) in 200 ml distilled water. The initial pH value of solution was measured as 6. Then one to two drops of HCl were added to the solution in order to prevent the formation of zinc hydroxide. The starting solution was atomized at a frequency of 1.63 MHz by an ultrasonic nebulizer and using dry air. These films show wurtzite crystal structure with 80% optical transmittance. Krunks et al. [5] studied highly structured ZnO layers comprising well-shaped hexagonal rods prepared by spray pyrolysis deposition of zinc chloride aqueous solutions in the temperature range of 490–560 °C. The precursor solution was pulverized onto the substrates placed on a soldered tin bath. Also they show a flat ZnO film evolves into the structured layer consisting of single crystalline hexagonal elongated prisms at growth temperatures close to 500 °C and above. According to them, the size of rods on glass substrates is increased by the growth temperature and solution concentration, leading to decreased *c*-axis orientation and lower substrate coverage. Zhao et al. [6] studied the comparison of structural and photoluminescence properties of ZnO thin films grown by pulsed laser deposition and ultrasonic spray pyrolysis on to the highly resistive p-type Si (1 0 0) wafers, which were etched with diluted HF (10%) for 3 min before being loaded into the growth chamber. They concluded that the ZnO film grown by PLD exhibits better crystallinity than that grown by USP. Bacaksiz et al. [7] revealed deposition of zinc oxide

* Corresponding author. Tel.: +91 231 2609435; fax: +91 231 2691533.
E-mail address: rajpure@yahoo.com (K.Y. Rajpure).

0925-8388/$ – see front matter © 2010 Elsevier B.V. All rights reserved.
doi:10.1016/j.jallcom.2010.05.019

thin films with zinc chloride as precursor onto the quartz substrate at 550 °C using spray pyrolysis method and subsequently annealed between 600 °C and 900 °C with a step of 100 °C. They concluded that XRD and SEM images indicate the annealing temperature did not play a great role on the microstructure of ZnO films and very less transmittance ~25%. Rao et al. [8] showed the effect of stress on the optical band gap of zinc oxide thin films with various substrate temperature by spray pyrolysis zinc acetate as a precursor, prepared by dissolving in a mixture of deionized water and ethanol. In this mixture, ethanol concentration was 10 ml in 100 cm^3 solution. The ZnO thin films were deposited at substrate temperatures of 350 °C, 400 °C, and 450 °C. They observed the grain growth and crystallinity of ZnO thin films increases with substrate temperature. The XRD studies show that the films deposited at low temperature (350 °C) have large stress, which relaxes as the temperature of the substrate is increased. Breedon et al. [9] reported the interconnected growth of ZnO nanowires in a two-stage process, using spray pyrolysis, deposited ZnO seed layers as a nucleation platform for subsequent hydrothermal growth. In this two-stage process, ZnO seed layers were first deposited onto rotating glass substrates at 450 °C using a typical spray pyrolysis deposition system. The precursor solution (100 cm^3) was prepared by dissolving 0.15 M of zinc acetate dihydrate in a solvent mixture of double deionized water and isopropyl alcohol with a 1:3 volume ratio. To enhance the solubility of zinc acetate, 0.4 cm^3 of acetic acid was also added to the solution. They present a comparison between the effect of these spray pyrolysis deposited seed layers and well-ordered sputter deposited seed layers, along with their respective ZnO nanomorphologies that were obtained via hydrothermal growth. Li and Haneda [10] synthesized the ZnO powders with different morphologies by alkali precipitation, organo-zinc hydrolysis, and spray pyrolysis. A 0.05 M zinc acetate aqueous solution was atomized by a nebulizer and then passed through a high temperature quartz tube under the suction of an aspirator. The pyrolysis proceeded quickly as droplets passed through the quartz tube at high temperature within a second. The formed ZnO powder was collected with a glass filter installed at the end of the quartz tube. The dependence of the photocatalytic activity on crystallinity, surface area, and particle morphology or acetaldehyde adsorptivity is discussed. Ghimbeu et al. [11] reported the preparation of zinc oxide thin films by zinkacetat-dehydrate precursor on platinum coated alumina substrate with ethanol as a solvent using electrostatic spray deposition technique for NO_2 gas sensor application. Various deposition techniques have been widely used to produce zinc oxide thin films. However, seeking the most reliable and economic deposition technique is the main goal. The most intensively studied techniques include, RF magnetron sputtering [12], thermal evaporation [13], sol–gel method [14], pulsed laser deposition (PLD) [15,16] and spray pyrolysis [17–19]. Among these methods, spray pyrolysis is the most useful technique for large area applications. This method is cheaper, simple and allows us to obtain films with high transparency and conductivity for optoelectronic applications. Many authors have extensively investigated zinc oxide thin films by CSP [20–26]. However, all of them have used a mixture of water and harmful toxic acids, alcohols, etc. as solvents for preparing spraying solution. Preparation of non-toxic, cost-effective and good stable material is the need of society and its use in optoelectronic devices alternative to CdO, SnO_2, In_2O_3 is necessity of nature.

The aim of our present work is to examine the significance of pre-heating temperature on surface morphology and crystallinity of the films, by virtue of their ability to act as platelets. In addition to that, we studied the role of morphology or crystallinity on the contact angle and optoelectronic properties. We have demonstrated a soft chemical route that enabled the formation of the compact, large effective (photoactive) surface area and defect free zinc oxide thin film electrodes, suitable for PEC solar cells.

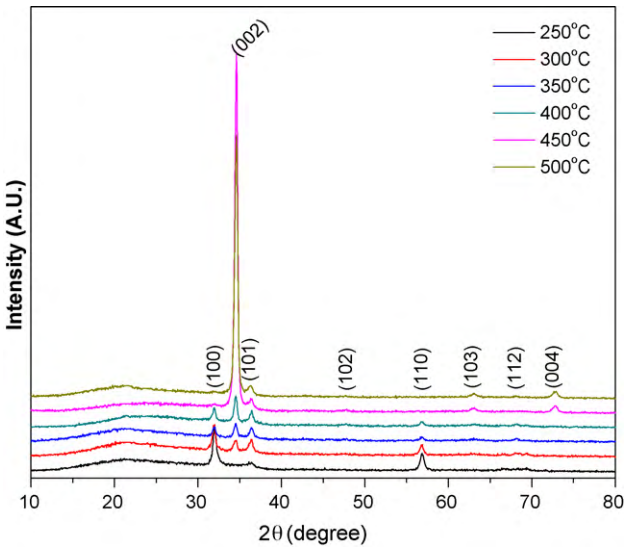

Fig. 1. X-ray diffraction patterns of zinc oxide thin films prepared at different pre-heating temperatures at optimized concentration of 0.5 M.

2. Experimental

Highly transparent and conducting *c*-axis oriented zinc oxide thin films were synthesized using chemical spray pyrolysis technique onto the ultrasonically and chemically cleaned corning glass substrates. The 0.5 M zinc acetate ($Zn(CH_3COO)_2{\cdot}2H_2O$) Aldrich, 99.99%, A.R. grade is dissolved in double distilled water. The resulting 50 cm^3 solution was sprayed onto cleaned corning glass substrates for different pre-heated temperatures assisted with compressed air as a carrier gas. The fine aerosols of aqueous zinc acetate solution after being sprayed through an atomizer onto the preheated glass substrate underwent pyrolytic decomposition, forming thereby a thin solid film. Other preparative parameters viz., solution concentration (0.5 M), spray rate (5 cm^3/min), nozzle to substrate distance (32 cm) were kept constant for all experiments.

The structural characterization of deposited thin films were carried out, by analyzing the X-ray diffraction patterns obtained under Cu-K_α (λ = 1.5406 Å) radiation from a Philips X-ray diffractometer model PW-1710 and surface morphology was studied using JEOL JSM-6360 scanning electron microscope (SEM). The surface topography of thin films was also analyzed from the AFM images taken by means of the atomic force microscope (Nanoscope instruments, USA) in the contact mode. The hydrophobicity of the films was tested by measuring the contact angle (θ) of a water droplet of 2.4 mm diameter placed on the film surface using the contact angle meter equipped with a CCD camera (Ramehart Instrument Co., USA) at a ambient temperature. The resistivity of the film was measured using Hall effect technique in van der Pauw configuration. Transmission spectra were recorded at room temperature and near to normal incidence using a Jobin–Yvon monochromator, a goniometric set-up, a UV-enhanced photodiode (Hamamatsu) and lock-in amplification. Thicknesses were computed using surface profiler of all thin films. The photoelectrochemical study was performed in a conventional three-electrode arrangement with the deposited thin film as working electrode, a graphite counter electrode and an SCE reference electrode. A 0.5 M NaOH aqueous solution is used as an electrolyte. The photoelectrochemical (PEC) characteristics were measured under constant illumination from a 25 W UV lamp with excitation wavelength of 365 nm.

3. Results and discussion

Fig. 1 shows the X-ray diffraction (XRD) patterns of zinc oxide thin films deposited at various substrate temperatures. The films are polycrystalline and fit well with the hexagonal (wurtzite) crystal structure with highly preferred orientation along (0 0 2) plane. Comparison of standard and observed '*d*' values of zinc oxide thin films deposited for various temperatures is shown in Table 1. The reason for relatively lower peak intensities is the formation of amorphous plus nanocrystalline phase in thin films. Big hump in the X-ray diffraction pattern around 14–25° angles is the evidence for this. The films are segregated into grain boundaries to inhibit the crystallization and preferred orientation of zinc oxide. The data is analyzed by making use of Joint Committee for Powder

Table 1
Comparison of standard and observed '*d*' values for zinc oxide films at various temperatures.

(*h k l*) planes	Standard '*d*' values (Å)	Comparison of standard and observed '*d*' values for zinc oxide films					
		250 °C	300 °C	350 °C	400 °C	450 °C	500 °C
(1 0 0)	2.816	2.8168	2.8031	2.8108	2.8138	2.8134	2.8140
(0 0 2)	2.602	2.6016	2.5950	2.6016	2.5993	2.6017	2.5995
(1 0 1)	2.476	2.4761	2.4701	2.4764	2.4744	2.4751	2.4755
(1 0 2)	1.911	1.9129	1.9087	1.9095	1.9107	1.9147	1.9142
(1 1 0)	1.626	1.6223	1.6228	1.6218	1.6235	1.6250	1.6265
(1 0 3)	1.477	1.4770	1.4740	1.4769	1.4778	1.4757	1.4754
(1 1 2)	1.379	1.3785	1.3763	1.3778	1.3778	1.3785	1.3768
(0 0 4)	1.301	1.310	1.2995	1.3024	1.3011	1.3026	1.3029

Diffraction Standards (JCPDS) card No. 05-0664. As the temperature increases, the intensity of (1 0 0) and (1 1 0) planes decreases and that of (0 0 2) plane increases evidently, showing the crystal reorientation effect. Also slight increase in intensity of (1 0 1), (1 0 3) and (0 0 4) is observed. Some weak reflections such as (1 0 2), (1 1 0), (1 0 3), (1 1 2) and (0 0 4) have also been observed but with small intensities. As the temperature increases, weak reflections almost disappears and highly *c*-axis oriented films resulted. No extra phases (such as Zn, ZnOH, etc.) corresponding to other oxides are detected even at different temperatures. The diffraction angle of the (0 0 2) peak is almost in agreement with the zinc oxide bulk single crystal, implying that no evident residual stress or inclusion-induced lattice distortion has been developed in the film due to temperature. The thermal oxidation process of ZnO may be described as follows: due to the existence of environmental oxygen, the oxidation begins at the surface of the Zn particles; ZnO phase is nucleated and formed as dispersed clusters on the surface of the Zn particles.

The crystallite size of the films is calculated using the Scherrer's formula applied to the (0 0 2) orientation which is maximum intensity reflection of structure ($2\theta = 34.15^\circ$),

$$D = \frac{0.9\lambda}{\beta \cos\theta} \quad (1)$$

where λ is the wavelength of Cu-K_α line, β is FWHM in radians and θ is the Bragg's angle. The crystallite size, calculated along (0 0 2) direction of the zinc oxide film is in the range of 60–100 nm. The crystallite size decreases up to 450 °C temperature and then increases for higher deposition temperatures. Quantitative information concerning the preferential crystallite orientation is obtained from different texture coefficients (*h k l*) defined by well known relation,

$$\mathrm{TC}(h\ k\ l) = \frac{I(h\,k\,l)/I_0(h\,k\,l)}{(1/N)\sum_N I(h\,k\,l)/I_0(h\,k\,l)} \quad (2)$$

where $I(h\,k\,l)$ is measured intensity, $I_0(h\,k\,l)$ is the JCPDS (card No. 05-0664) intensity and N is the reflection number. It is seen that texture coefficient of (0 0 2) plane increases suddenly with temperatures. The highest achieved value of texture coefficient at (0 0 2)

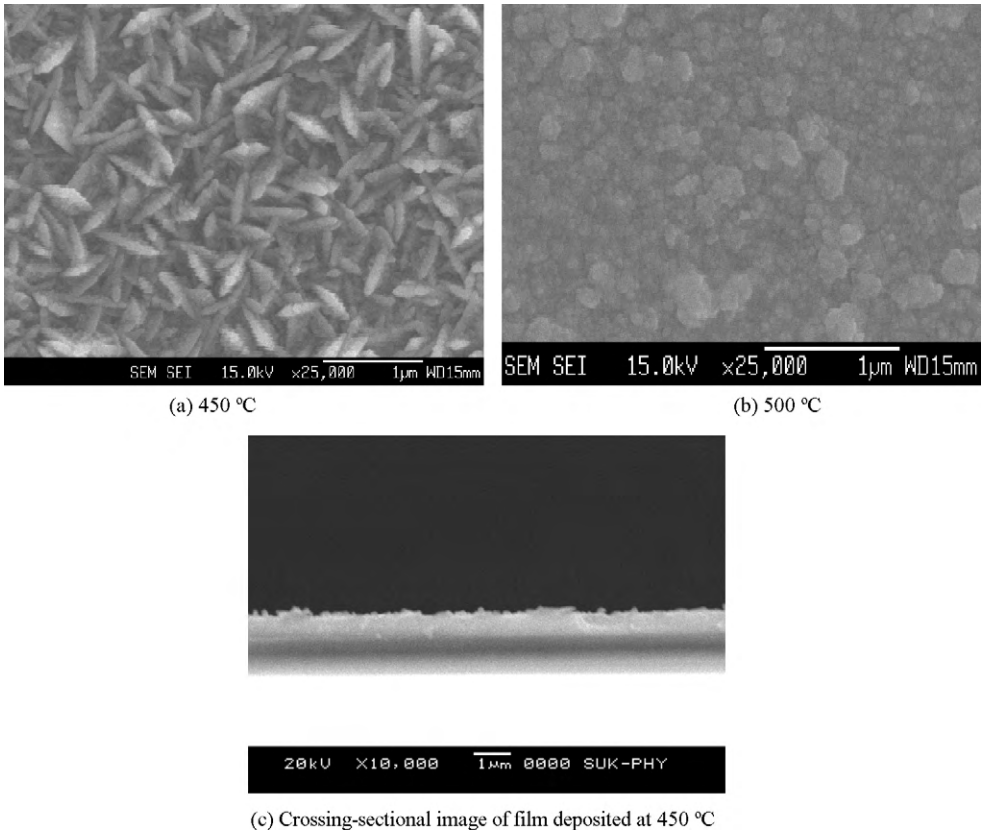

(a) 450 ºC

(b) 500 ºC

(c) Crossing-sectional image of film deposited at 450 ºC

Fig. 2. Scanning electron micrographs of zinc oxide thin films prepared at (a) 450 °C, (b) 500 °C, and (c) cross-sectional image of film deposited at 450 °C.

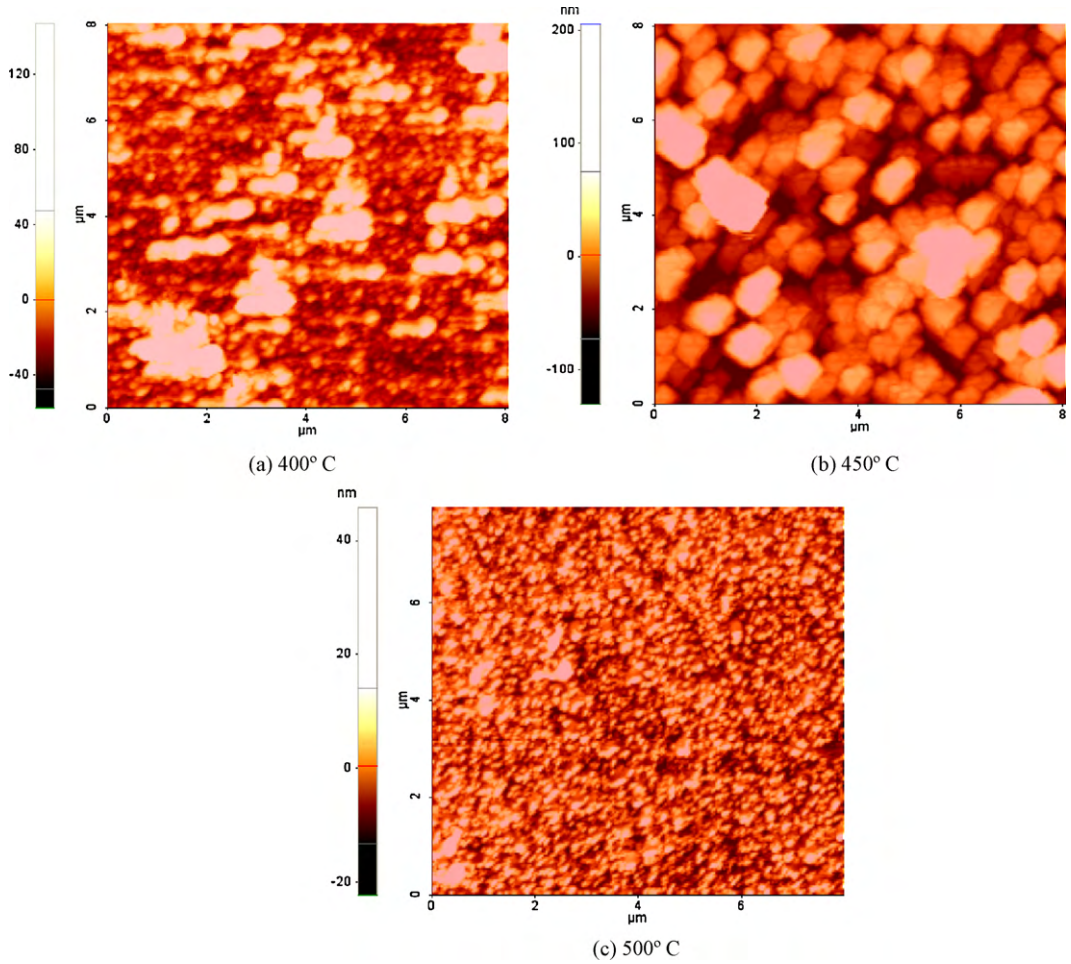

Fig. 3. 2D atomic force micrographs of zinc oxide thin films prepared at (a) 400 °C, (b) 450 °C, and (c) 500 °C with 1 μm × 1 μm planar.

plane is 5.8 at 450 °C temperature due to enhancement in the crystallinity of the lattice. The strain generated in our films is calculated using relation [27],

$$\beta = \frac{\lambda}{D\ \cos\theta} - \varepsilon\ \tan\theta \tag{3}$$

where β is the FWHM, $\lambda = 1.5406$ Å is the wavelength of the Cu-K_α radiation, θ is the Bragg angle, D is the crystallite size, and ε is the stain. As the temperature increases strain decreases from 5.67×10^{-3} to 1.44×10^{-3} along the (0 0 2) plane due to enhancement in sharpness of planes. For solar cell applications, a smaller particle size is desirable as it provides a greater surface area for conduction mechanism leading to an enhancement in efficiency.

Scanning electron micrographs (SEM) of zinc oxide thin films deposited at different substrate temperatures are shown in Fig. 2. Hexagonal platelets are seen in the micrograph deposited at 450 °C temperature on the film surface. These faceted grains of the film are densely agglomerated and show preferential growth orientation along (0 0 2) plane. The textured morphology is a consequence of the nucleation of *c*-axis oriented grains that grow geometrically and impinge laterally. As the grains agglomerated with an increase in the temperature, large flake-like structure is observed in the films. It is observed that the grain size (~100–150 nm) observed by SEM images is larger than the value determined by XRD, which may be due to the discrepancy between the mean dimension of the crystallites perpendicular to diffracting planes by XRD diffraction and the observable aggregates in SEM images. Cross-sectional view of the film deposited at 450 °C is shown in Fig. 2c. In addition to flakes, the overgrown aggregates of spherical particles at 500 °C as seen in figure. Therefore it can be concluded that the morphology of the particles are changed and their sizes are reduced by increasing the reaction temperature. There are two possibilities associated with the phenomena. One is the effect from outside and the other from inside. It is known that the oxygen and vapour in the air would have big effect on the morphology. When the exchange of oxygen between grains and air happens, the collapse may happen. We tend to agree with the second mechanism that the collapse is probably due to the strain release of crystallites due to high temperature. The formation of 3D crystallites is mainly governed by surface energy, elastic strain and surface diffusion kinetics. Theoretically, small regions of high strain will evolve as grooves or pits if strain is not homogeneously relieved during the growth [28]. Therefore, we can assume that the uneven component distribution of ZnO which grown at relatively low temperatures could result in local sites with high strain. As a result, the depositing materials diffused away from these high-strain sites, leaving behind the pits on the surface.

Fig. 3 shows the two-dimensional atomic force microscopy (AFM) images of zinc oxide thin films deposited for different preheating temperatures. The images are recorded on 1 μm × 1 μm planar in contact mode at the scan rate of 10.17 Hz. The films show compact and dense pinhole free hexagonal platelets like structure correlated with SEM images. At higher temperature, the atoms have enough activation energy to occupy the correct lattice sites in the crystal lattice and grains with lower surface energy become larger. Sprayed zinc oxide films exhibit hexagonal structure with preferred orientation growth along (0 0 2) plane becomes strong and leads to an improvement in the crystallinity. RMS surface roughness is 40, 25 and 14 for 400 °C, 450 °C, 500 °C samples, respectively.

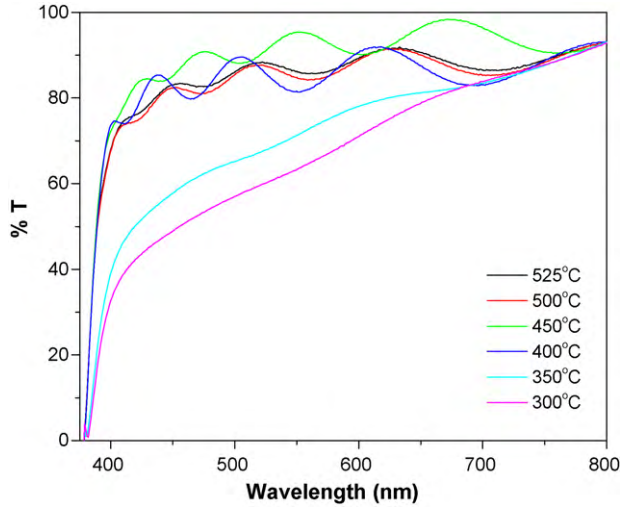

Fig. 4. Variation of transmittance (T) with wavelength for spray deposited zinc oxide thin films deposited at different temperatures.

Wettability of the films was evaluated by measuring static contact angles for water. The change in water contact angle values as a function of pre-heating temperature is shown in Table 1. All films show the hydrophilic behaviour. The water contact angle value increases from 58° to 76° with increase in temperature from 250 °C to 450 °C is due to the fact that, the surface roughness of the film decreases with increase in temperature. However, with further increase in temperature (500 °C), the water contact angle value slightly decreases to 67°. This is due to the fact that, at 500 °C the film shows increase in surface roughness. The wettability of the film surface is mainly influenced by the chemical composition and surface morphology. It is confirmed from SEM figure that, the films having temperature at 300 °C, shows hexagonal platelets like structure on which the water contact angle shows 61°. The films having temperatures 400 °C and 450 °C reveals increase in compactness of the surface leading to increase in water contact angle from 67.5° and 76°, respectively. The compact microstructure of the film surface shows higher water contact angle values as compared to smooth one. The reason for this behaviour may be that for high roughness gas bubbles are embedded between the water drop and the insulator surface [29,30]. These samples are highly applicable to increase lifetime of solar cells and used in defrosters and transparent window coatings.

Fig. 4 shows the optical transmission spectra of ZnO films recorded in the wavelength range 350–850 nm. The well-developed interference patterns in T show that the films are specular to a great extent. The decrease in transmittance at higher temperature (>450 °C) may be due to the increased scattering of photons by crystal defects. The free carrier absorption of photons may also contribute to the reduction in optical transmittance [31]. An increase in the transmittance of zinc oxide films can be attributed to the removal of organic and hydroxide species on the film. Interestingly, 450 °C sample exhibited increased optical transmission in the visible region and this is good for device application. In transparent metal oxides, the metal to oxygen ratio decides the percentage of transmittance. A metal-rich film usually exhibits less transparency [32]. The amplitude of interference fringes decreased for higher temperatures (>450 °C) and this indicated the loss in surface smoothness leading to a slight scattering loss. The typical transmittance of the annealed films at 550 nm wavelength is of the order of 95%. Such films would have potential applications in opto-electronic devices. The spectra clearly exhibit a slight blue shift in band edge due to the variation of substrate temperature, with a transparency in the visible range. The band gap of films increases after 350 °C temperature showing negative strain along c-axis. So the blue shift of the band gap is attributed to the compressive strain in deposited zinc oxide films and after increasing the deposition temperature the band-gap value is decreasing due to the relaxation of the built in strain.

The figure of merit (ϕ) of the film plays an significant role in optoelectronic device applications is determined using the formula,

$$\phi = \frac{T^{10}}{R_s} \tag{4}$$

where T is transmittance at 550 nm wavelength and R_s the sheet resistance.

Figure of merit (ϕ) of deposited thin films increases with increase in temperature and achieved highest figure of merit 7.88×10^{-4} □/Ω at 450 °C, which is highest value as per the authors knowledge for pure zinc oxide thin films.

The dependence of electrical resistivity of all films with various pre-heating temperatures is shown in Table 2. The initial decrease in resistivity with temperature up to 450 °C is a consequence of increase in mobility which is found to increase due to the improvement of the crystalline structure of the films due to heating as observed by the XRD analysis. With increased crystallinity, grain size increases thereby minimizing the grain boundary scattering losses and defects in the annealed films. So the number of electron trap states reduces and hence the carrier concentration increases. Further, the resistivity increases after 450 °C temperature due to evaporation of solution and slightly generation of powdery films. Since air and water are, respectively, used as the carrier gas and solvent, there might have been the possibility of chemisorptions of oxygen during deposition of the films. Zinc oxide is an n-type semiconductor in which donor levels are due to oxygen vacancies V_O and interstitial zinc Z_{ni} atoms. Hence one can assume that, the reason for decrease in resistivity may be due to creation of oxygen vacancies V_O and zinc interstitial Z_{ni} during the deposition.

For the zinc oxide films deposited at various temperatures, under UV illumination in terms of open circuit voltage (V_{oc}) and short circuit current (I_{sc}) are presented in Table 2. In dark and under illumination current–voltage (I–V) characteristics of glass/fluorine doped tin oxide/zinc oxide/SCE cells were measured. The efficiency (η%) and Fill factor are calculated from the relations,

$$\eta(\%) = \frac{V_{oc} I_{sc} FF}{P_{input}} \times 100 \tag{5}$$

$$FF = \frac{I_{max} V_{max}}{I_{sc} V_{oc}} \tag{6}$$

Table 2
Various parameters of spray deposited zinc oxide thin films at different pre-heating temperatures.

Sub. Temp. (°C)	R_s (kΩ/□)	% T at 550 nm	Resistivity, ρ (Ω cm)	Angle of contact (deg)	Fig. of merit, Φ ($\times 10^{-4}$) (□/Ω)	I_{sc} (μA)	V_{oc} (mV)
250	150	60.25	9.68	57.80	0.00042	72	217
300	35	63.37	2.54	61.2	0.002986	98	255
350	25	71.39	1.89	63.56	0.01376	122	280
400	12.5	81.58	0.96	67.52	0.1045	157	315
450	0.8	95.49	0.062	75.94	7.8810	212	353
500	2	84.89	0.161	66.77	0.97227	160	305

where P_{input} is the input light intensity, I_{max} and V_{max} are the values of maximum current and maximum voltage, respectively that can be extracted from a PEC solar cell. From *I–V* measurements it is observed that the higher magnitude of I_{sc} = 212 μA, V_{oc} = 353 mV, *FF* = 0.32 and η = 1.64% are obtained for the films deposited at 450 °C using NaOH as an electrolyte. The compact and densely packed ZnO hexagonal crystallites can absorb enough light. Furthermore, the photogenerated electrons can transport directly through hexagonal crystallites and compact layers to the conducting substrates with minimum loss. This greatly reduces the recombination losses of photogenerated charge carriers due to decrement in grain boundary resistance in the charge transportation process.

4. Conclusions

Highly transparent and conductive zinc oxide thin films of hexagonal crystallites are synthesized on to the corning glasses by spray pyrolytic decomposition in presence of various temperatures. The films are found to be highly preferred *c*-axis oriented perpendicular to the substrate, which confirmed from the XRD and surface micrographs. Films show the hydrophilic nature. Compact hexagonal platelets like structure is observed for lower temperature sample. The films exhibit nanoparticles of size 60–100 nm for 250–500 °C temperatures. Films are highly transparent and conducting, we achieved 95% transmittance at 550 nm with electrical resistivity 0.062 Ω cm and figure of merit 7.88×10^{-4} □/Ω. Moreover samples are photoelectrochemically active and exhibit the highest photocurrent of 212 μA, a photovoltage of 353 mV, 0.32 fill factor and 1.64% efficiency for the 450 °C films. These zinc oxide films synthesized at optimized deposition conditions are good alternative candidate for potential applications in thin film solar cells and as window coatings for increasing the lifetime of device.

Acknowledgement

S.S. Shinde is thankful to Defence Research and Development Organization (DRDO), New Delhi for its financial support.

References

[1] D.M. Bangall, Y.F. Chen, Z. Zhu, T. Yao, S. Koyama, M.Y. Shen, T. Goto, Appl. Phys. Lett. 70 (1997) 2230.
[2] V. Hagiwara, T. Nakada, A. Kunioka, Sol. Energy Mater. Sol. Cells 67 (2001) 267.
[3] B. Sang, A. Yamada, M. Konagai, Jpn. J. Appl. Phys. 37 (1998) L206.
[4] U. Alver, T. Kılınç, E. Bacaksız, T. Küçükömeroğlu, S. Nezir, İ.H. Mutlu, F. Aslan, Thin Solid Films 515 (2007) 3448.
[5] M. Krunks, T. Dedova, I. Oja Açik, Thin Solid Films 515 (2006) 1157.
[6] J.L. Zhao, X.M. Li, J.M. Bian, W.D. Yu, C.Y. Zhang, Thin Solid Films 515 (2006) 1763.
[7] E. Bacaksiz, S. Yılmaz, M. Parlak, A. Varilci, M. Altunbas, J. Alloy Compd. 478 (2009) 367.
[8] T.P. Rao, M.C. Santhosh Kumar, S.A. Angayarkanni, M. Ashok, J. Alloy Compd. 485 (2009) 413.
[9] M. Breedon, M.B. Rahmani, S. Keshmiri, W. Wlodarski, K. Kalantar-zadeh, Mater. Lett. 64 (2010) 291.
[10] D. Li, H. Haneda, Chemosphere 51 (2003) 129.
[11] C.M. Ghimbeu, J. Schoonman, M. Lumbreras, M. Siadat, Appl. Surf. Sci. 253 (2007) 7483.
[12] J. Krc, M. Zeman, O. Kluth, F. Smole, M. Topic, Thin Solid Films 426 (2003) 296.
[13] S.A. Aly, N.Z. Elsayed, M.A. Kaid, Vacuum 61 (2001) 1.
[14] J.-H. Lee, K.-H. Ko, B.-O. Park, J. Cryst. Growth 247 (2003) 119.
[15] J.-M. Myoung, W.-H. Yoon, D.-H. Lee, I. Yun, S.-H. Bae, S.-Y. Lee, Jpn. J. Appl. Phys. 41 (2002) 28.
[16] H.-J. Ko, T. Yao, Y. Chen, S.-K. Hong, J. Appl. Phys. 92 (2002) 4354.
[17] S. Major, A. Banerjee, K.L. Chopra, Thin Solid Films 108 (1983) 333.
[18] S.A. Studenikin, N. Golgeo, M. Cocivera, J. Appl. Phys. 83 (1998) 2104.
[19] C. Falcony, A. Ortiz, M. Garcia, J.S. Helman, J. Appl. Phys. 63 (1988) 2378.
[20] P.M. Ratheesh Kumar, C. Sudha Kartha, K.P. Vijayakumar, F. Singh, D.K. Avasthi, T. Abe, Y. Kashiwaba, G.S. Okram, M. Kumar, Sarvesh Kumar, J. Appl. Phys. 97 (2005) 013509.
[21] M.Y. Ge, H.P. Wu, L. Niu, J.F. Liu, S.Y. Chen, P.Y. Shen, Y.W. Zeng, Y.W. Wang, G.Q. Zhang, J.Z. Jiang, J. Cryst. Growth 305 (2007) 162.
[22] Y.L. Wu, A.I.Y. Tok, F.Y.C. Boey, X.T. Zeng, X.H. Zhang, Appl. Surf. Sci. 253 (2007) 5473.
[23] M. Dutta, S. Mridha, D. Basak, Appl. Surf. Sci. 254 (2008) 2743.
[24] A.E. Kandjani, M.F. Tabriz, B. Pourabbas, Mater. Res. Bull. 43 (2008) 645.
[25] L. Chen, Z.Q. Chen, X.Z. Shang, C. Liu, S. Xu, Q. Fu, Solid State Commun. 137 (2006) 561.
[26] F. Qu, D.R. Santos, N.O. Dantas, A.F.G. Monte, P.C. Morais, Physica E 23 (2004) 410.
[27] J.B. Nelson, D.P. Riley, Proc. Phys. Soc. Lond. 57 (1945) 160.
[28] Z. Gong, Z.C. Niu, Z.D. Fang, Z.H. Miao, S.L. Feng, Appl. Phys. Lett. 86 (2005) 013104.
[29] R.N. Wenzel, Ind. Eng. Chem. 28 (1936) 988.
[30] A.B.D. Cassie, S. Baxter, Trans. Faraday Soc. 40 (1944) 546.
[31] P.M.R. Kumar, C.S. Kartha, K.P. Vijayakumar, T. Abe, F. Singh, D.K. Avasthi, Semicond. Sci. Technol. 20 (2005) 120.
[32] H.L. Hartnagel, A.L. Dawar, A.K. Jain, C. Jagadish, Semiconducting Transparent Thin Films, Institute of Physics Publishing, Bristol, 1995, p. 244.